Subject: Detailed Responses to Reviewers: Liu, H., Maghoul, P., and Shalaby, A.: Seismic physics-based characterization of permafrost sites using surface waves, The Cryosphere Discuss. [preprint], `https://doi.org/10.5194/tc-2021-219`, in review, 2021.

Date: November 15, 2021

The authors are grateful for the valuable comments and kind consideration of our submission. Detailed responses and revisions based on these comments are listed below.

1 General Comments

This paper reports on the inversion of the dispersion curves from two types of seismic waves propagating in permafrost, to evaluate soil properties via a three-phase analytical model that accounts for the porosity and mechanical properties in the three layers. I think this paper is well written and is of interest for the audience of the Cryosphere. The findings are convincing, and in my opinion the paper deserves publication after the comments listed below have been considered.

For a non-specialist of permafrost-related studies, it would be beneficial that the authors provide a more systematic comparison of their approach with already existing methods. The main novelty here is the fact that the forward model includes new parameters (such as porosity, and the degree of ice saturation), and that the two waves are sensitive to different sets of parameters, which allows a separate inversion instead of a joint inversion. This should be emphasized by citing previous investigations of permafrost with seismic methods, and by checking that the parameters are consistent with other similar studies, when possible.

Currently, the existing models predominately apply an elastic approach as the forward solver in the dispersion analysis for permafrost sites. Our proposed model, on the other hand, uses a hybrid inverse and multi-phase poroelastic approach for the characterization of permafrost sites. In the existing methods that are used for the inversion analysis of MASW measurements for permafrost sites, it is commonly considered that the permafrost layer (frozen soil) is associated with a higher shear wave velocity due to the presence of ice in comparison to the unfrozen ground (Dou et al, 2014, Glazer et al, 2020). However, the porosity and soil type can also significantly affect the shear wave velocity (Liu et al, 2020). In other words, a relatively higher shear wave velocity could be associated with an unfrozen soil layer with a relatively lower porosity or stiffer solid skeletal frame, and not necessarily related to the presence of a frozen soil layer. Therefore, the detection of the permafrost layer from only the shear wave velocity may lead to inaccurate and even misleading interpretations.

Here, we present a hybrid inverse and multi-phase poromechanical approach for physics-based in-situ characterization of permafrost sites using surface wave techniques. In our method, we quantify the physical properties such as ice content, unfrozen water content, and porosity as well as the mechanical properties such as the shear modulus and bulk modulus of permafrost or other soil layers. The amount of ice content can be used, rather than the shear wave velocity, to explicitly indicate the active layer, permafrost and unfrozen ground. The role of two different types of Rayleigh waves in characterizing the permafrost is presented based on an MASW seismic investigation in a field located at SW Spitsbergen, Svalbard. As mentioned in your comment, the objective is to use a separate inversion instead of a joint inversion. Glazer et al, 2020 performed both seismic surveys (MASW test) and electrical resistivity investigations at the site in September 2017 to study the evolution and formation of permafrost considering surface watercourses and marine terrace. In our study, the same experimental data collected by Glazer et al, 2020 is used to demonstrate the inversion analysis based on R1 and R2 Rayleigh waves.

In the revised manuscript, the comparison of the inversion results using the proposed hybrid inverse and multi-phase poro-mechanical approach and inversion results from the ERT survey provided by Glazer et al., (2020) has been added. It was reported by Glazer et al., (2020) that the permafrost table is located at a depth of about 2 m for a span of 20 m investigated by the ERT survey. The new inversion results in terms of the thickness of the active layer were also validated using the results reported by Dobiński et al., (2010) and Dolnicki et al., (2013) by the direct probing method. It was also reported by Dobiński et al., (2010) and Dolnicki et al., (2013) that the active layer in Svalbard is approximately 1.65–2.5 m deep. The direct sampling results reported by Szymański et al. (2013) confirmed that the study site is very wet and the water table is very high (around 15 cm). It was reported by Szymański et al. (2013) that this study site also contains a lot of coarse sandy soils, gravels as well as around 20% silty clay based on the direct sampling methods at the top 15 cm. Our inversion results, as shown in Figure 1, predicted that the permafrost table is generally located at about 1.5-1.9 m below the ground surface, which is consistent with the ERT results reported by Glazer et al., (2020) and results reported by Dobiński et al., (2010) and Dolnicki et al., (2013) using the direct probing method.

Based on the field description of the testing site by Glazer et al., (2020), the unconsolidated sedimentary rock contains a high proportion of pore spaces; consequently, they can accumulate a large volume of pore-water or pore-ice. Our inversion results showed that the porosity of the active layer ranges from 0.56 to 0.69, which is consistent with the field description by Glazer et al., (2020). The unfrozen water content in the second permafrost layer was predicted ranging from 0.05-0.17. Li et al. (2020) and Zhang et al. (2020) showed that the residual volumetric unfrozen water content for silty-clay, clay, medium sand, and fine sand is 0.12, 0.08, 0.06 and 0.03, respectively. Our inversion results predicted that soils are mostly silty-clay or clay (Section 1-3) and sandy soils, which are also consistent with the results described by Szymański et al. (2013). Figure 1e shows the variation of the shear modulus of soil skeleton predicted by the proposed hybrid inverse and multi-phase poro-mechanical approach. The predicted shear modulus in the first layer at the offset distance of 0 to 360 m ranges from 4 GPa to 7.9 GPa, which represents clay soils (Helgerud et al. 1999). At the offset distance of 360 to 600 m, the estimated shear modulus in the first layer ranges from 27 GPa to 33 GPa, which corresponds to soils with calcite constituents (Helgerud et al. 1999). Calcite most commonly occurs in sedimentary rock or gravels (Schmid et al., 1987), which is consistent with the field description given by Glazer et al. 2020 and Szymański et al. (2013).

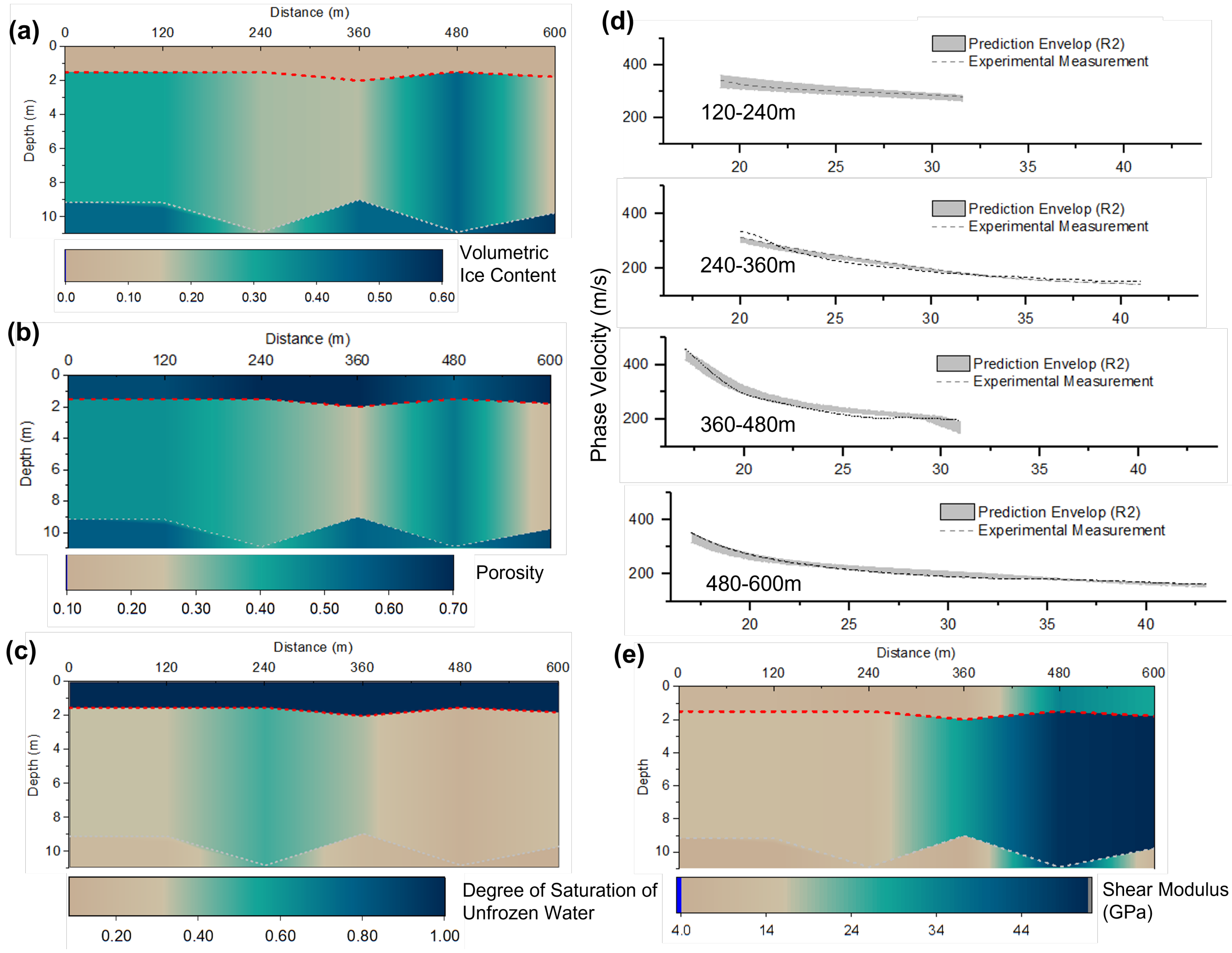

Figure 1: Summary of the inversion results at the offset distance from 0 m to 600 m. **(a)** Volumetric ice content distribution. **(b)** Soil porosity distribution. **(c)** Distribution of the degree saturation of unfrozen water. **(d)** Comparison between the numerical and experimental dispersion curves for R2 wave. **(e)** Distribution of the shear modulus of the solid skeletal frame.

Reference:

Dou, S., & Ajo-Franklin, J. B. (2014). Full-wavefield inversion of surface waves for mapping embedded low-velocity zones in permafrost. Geophysics, 79(6), EN107-EN124.

Glazer, M., Dobiński, W., Marciniak, A., Majdański, M., & Błaszczyk, M. (2020). Spatial distribution and controls of permafrost development in non-glacial Arctic catchment over the Holocene, Fuglebekken, SW Spitsbergen. Geomorphology, 358, 107128.

Liu, H., Maghoul, P., & Shalaby, A. (2020). Laboratory-scale characterization of saturated soil samples through ultrasonic techniques. Scientific reports, 10(1), 1-17.

Dobiński, W., & Leszkiewicz, J. (2010). Active layer and permafrost occurrence in the vicinity of the Polish Polar Station, Hornsund, Spitsbergen in the light of geophysical research. Problemy

Klimatologii Polarnej, 20, 129-142.

Dolnicki, P., Grabiec, M., Puczko, D., Gawor, L., Budzik, T., & Klementowski, J. (2013). Variability of temperature and thickness of permafrost active layer at coastal sites of Svalbard.

Szymański, W., Skiba, S., & Wojtuń, B. (2013). Distribution, genesis, and properties of Arctic soils: a case study from the Fuglebekken catchment, Spitsbergen. Polish Polar Research, 289-304.

Helgerud, M. B., Dvorkin, J., Nur, A., Sakai, A., & Collett, T. (1999). Elastic-wave velocity in marine sediments with gas hydrates: Effective medium modeling. Geophysical Research Letters, 26(13), 2021-2024.

Li, Z., Chen, J., & Sugimoto, M. (2020). Pulsed NMR measurements of unfrozen water content in partially frozen soil. Journal of Cold Regions Engineering, 34(3), 04020013.

Zhang, M., Zhang, X., Lai, Y., Lu, J., & Wang, C. (2020). Variations of the temperatures and volumetric unfrozen water contents of fine-grained soils during a freezing–thawing process. Acta Geotechnica, 15(3), 595-601.

2 Specific comments

It would be useful to have a map of Svalbard showing the location of the experiment and the seismic network, instead of figure 4a, which does not provide much information about the study.

A map of the testing site has been added in the paper, as shown in Figure 2.

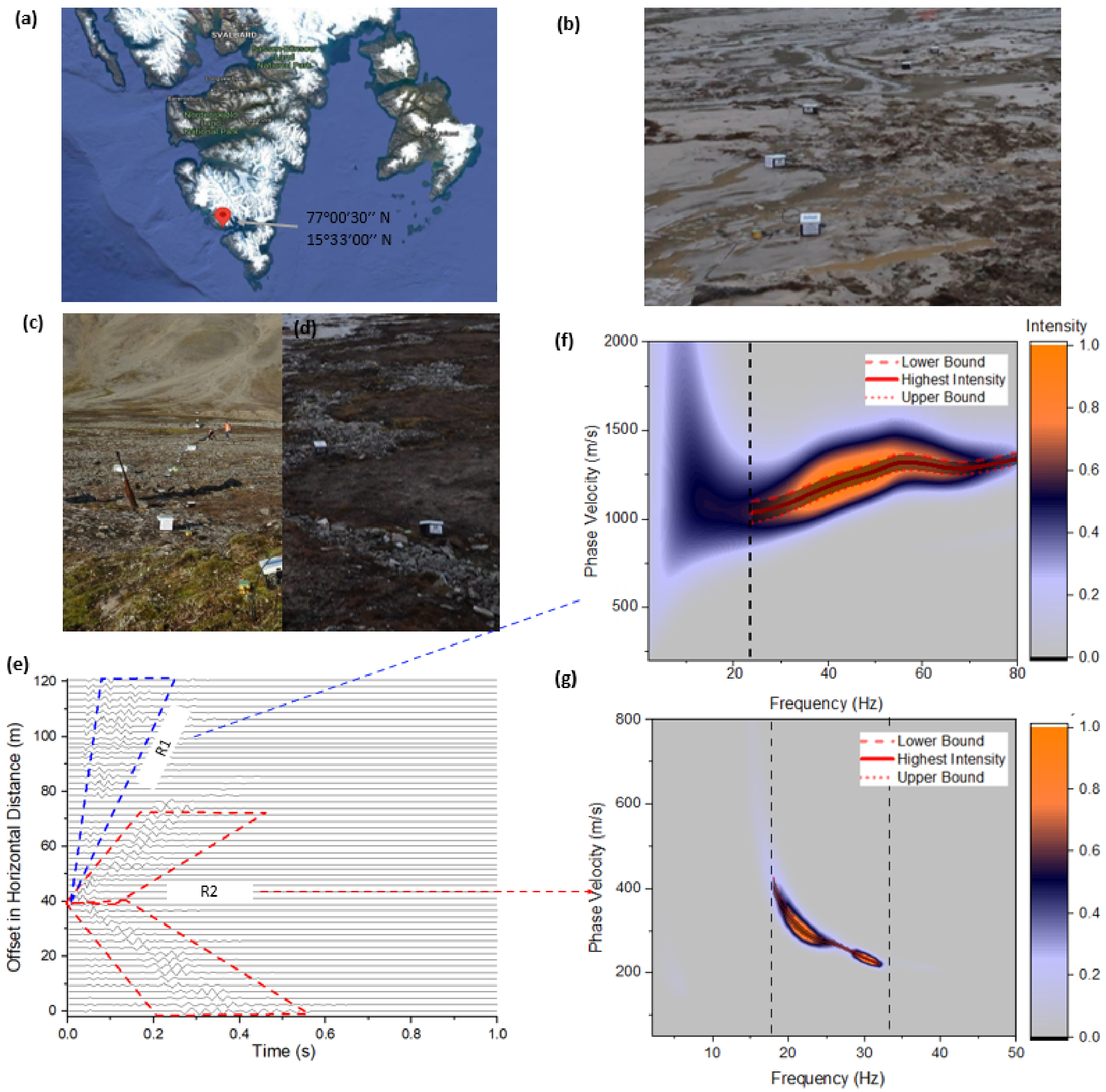

Figure 2: Surface wave measurement in Section 1 (from 0 m to 120 m). **(a)** Study area in Holocene, Fuglebekken, SW Spitsbergen. **(b)** Test site with clayey silt soils. **(c)** Test site with gravels and sands. **(d)** Test site with patterned ground. **(e)** Waveform data from the measurements at different offsets in horizontal distance. **(f)** Experimental dispersion image for R1 wave. **(g)** Experimental dispersion image for R2 wave

Section 3. There are many methods to extract dispersion curves from a shot gather. Please indicate which was used here.

The method used for the extraction of dispersion curves is the 'phase-shift method', which is implemented by the MASWave (Olafsdottir et al. 2018). In the revised manuscript, the dispersion curve is automatically selected initially based on the highest intensity in the dispersion spectra using MASWave software (Olafsdottir et al., 2018). The uncertainties due to the selection of the dispersion curve from the dispersion spectra have been considered in the revised manuscript. The dispersion curve is automatically selected initially based on the highest intensity in the dispersion spectra using MASWave software (Olafsdottir et al., 2018). Then a 90% confidence interval, as shown in Figure 2c and 2d), is considered to study the effect of the selection of dispersion curve on the inversion results.

Reference:

Olafsdottir, E. A., Erlingsson, S., & Bessason, B. (2018). Tool for analysis of multichannel analysis of surface waves (MASW) field data and evaluation of shear wave velocity profiles of soils. Canadian Geotechnical Journal, 55(2), 217-233.

Figure 4. I am not sure that the terminology employed to describe these two waves is adequate. The spectra look similar to those encountered when dealing with a mix between surface and guided waves, which are also created by the interference between P and S waves. Leaky guided waves are encountered in configurations where the layers have impedance discontinuities, for example sea ice on water, seismic waves in roads (a hard layer of bitumen resting on a soft substrate). Moreover, the R2 wave seems to have a cutoff frequency around 12 Hz, which indicates a higher-order mode. This needs clarifying. This could also be another explanation for the higher misfit in figure 7d. Have you checked the polarization of the two waves?

The guided waves are formed by interference of multiple reflections and mode conversion of compressional waves (P-waves) and shear waves (S-waves) at the two boundaries of the plate. The fundamental anti-symmetric mode (A0) and symmetric mode (S0) tend to converge to the same phase velocity (as described by Ryden & Park (2004)). The symmetric modes, also called longitudinal modes, are generated due to the wave propagation in the longitudinal direction. On the other hand, the antisymmetric modes are generated because of the wave propagation in the transverse direction (Graff 2012). In our study, the phase velocity of R1 and R2 does not converge to the same velocity since the generation of R1 or R2 as well as symmetric modes or antisymmetric modes are fundamentally different. The generation of R1 and R2 is due to the interaction of multiphase components (soil skeleton, unfrozen water and ice). We have proved that R1 waves appear due to the interaction of P1 and S1 waves. Similarly, R2 waves appear due to the interaction of P2 and S2 waves. However, the generation of anti-symmetric mode and symmetric mode is due to the geometry that constrains the wave propagation. The anti-symmetric mode and symmetric mode can be seen in solid materials. However, the R1 and R2 can only be generated in frozen soils with at least three phases.

The R2 wave at a range of 18-33 Hz is extracted from the original signal. Since the signal does not have clear low-frequency component, the exact cutting off frequency of R2 can not be determined. This has been discussed by Park et al. 2007. In their publication, dispersion curve shown in Figure 6 also shows a similar dispersion spectra where only dispersion curve after 18 Hz can be clearly identified (Park et al. 2007).

In our previous inversion analysis, we assumed that the last layer in our model is the unfrozen ground, which is indeed uncertain considering that the penetrating depth is only about 11 m in the MASW survey (based on the recommendation that MASW investigation depth is roughly half of the maximum wavelength (Olafsdottir et al., 2018)). For instance, the maximum wavelength in Section 1 is about 22 m (calculated using a phase velocity of 404 m/s at the frequency of 18 Hz). The maximum wavelength for Section 2 to 5 can be calculated in a similar manner. The average maximum wavelength for the entire investigation areas is around 21 m. Therefore, the penetrating depth in the MASW survey presented in this study is only about 11 m. It was reported that the permafrost layer in the studied site can go up to 100 m (Dolnicki et al., 2013; Glazer et al., 2018). Therefore, in the revised paper, we considered the last layer to have a degree of saturation of unfrozen water ranging from 1% to 99%. In this way, the last layer can be either permafrost or unfrozen ground. We have also applied the automatic methods for the selection of dispersion curves (instead of relying on visual inspection that we used in the original draft) using MASWave software (Olafsdottir, 2018). The misfits (RMS) between the R1 experimental and numerical dispersion curves at Section 4 have been significantly reduced from 49.6 to only 4.7 , as shown in Figure 3g.

Reference:

Park, C. B., Miller, R. D., Xia, J., & Ivanov, J. (2007). Multichannel analysis of surface waves (MASW)—active and passive methods. The Leading Edge, 26(1), 60-64.

Glazer, M., Dobiński, W., Marciniak, A., Majdański, M., & Błaszczyk, M. (2020). Spatial distribution and controls of permafrost development in non-glacial Arctic catchment over the Holocene, Fuglebekken, SW Spitsbergen. Geomorphology, 358, 107128.

Dolnicki, P., Grabiec, M., Puczko, D., Gawor, L., Budzik, T., & Klementowski, J. (2013). Variability of temperature and thickness of permafrost active layer at coastal sites of Svalbard.

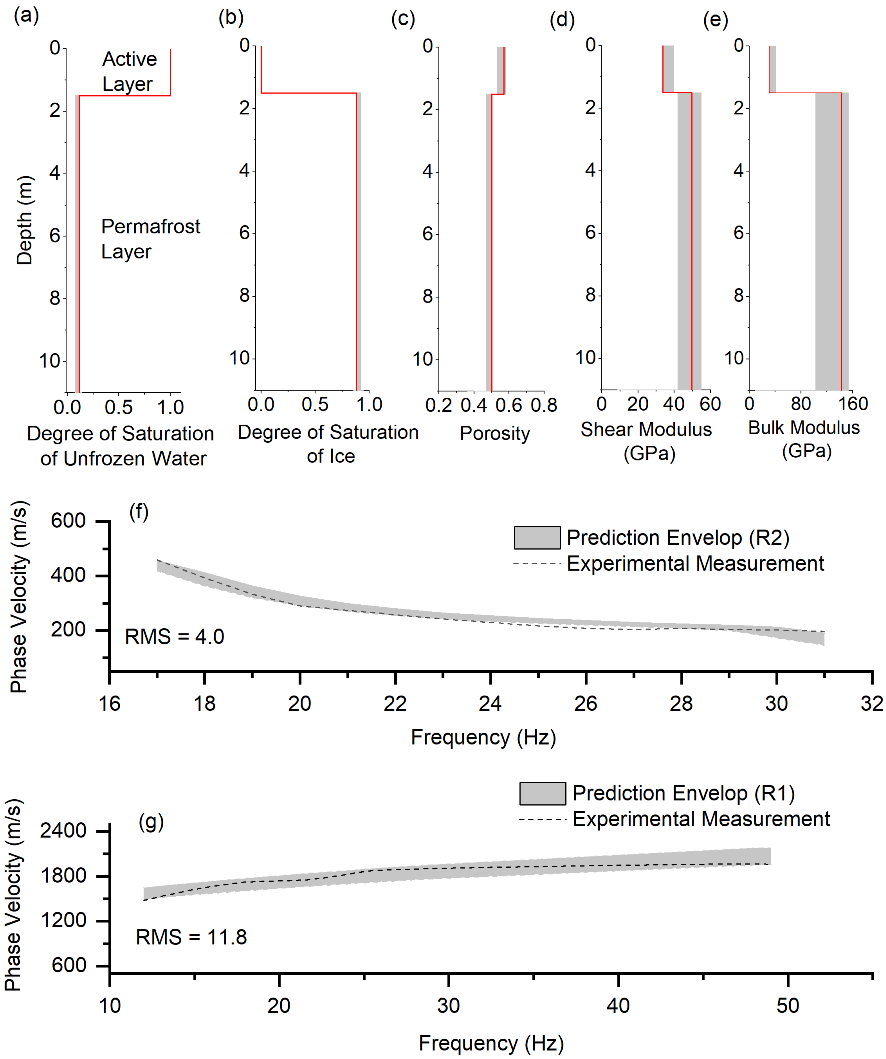

Figure 3: Surface wave inversion results for Section 4 (from 360m to 480m). **(a)** Degree of saturation of unfrozen water, **(b)** Degree of saturation of ice, **(c)** Porosity distribution, **(d)** Shear modulus of solid skeletal frame, **(e)** Bulk modulus of solid skeletal frame, **(f)** Experimental and numerical dispersion curves for R2 wave, **(g)** Experimental and numerical dispersion curves for R1 wave.

I do not see a direct transfer of this work to the applications mentioned in introduction and conclusion, such as ... the design of an early warning system for permafrost by means of an active or passive seismic test." we can also predict the soil type and the sensitivity of the permafrost layer to permafrost carbon feedback and emission of greenhouse gases to the atmosphere. These claims are a bit overreaching to me, because these remain to be proved. However, they could be mentioned as a follow-up to the present paper, with some guidelines on how to achieve these goals.

In this paper, our results demonstrate the potential of seismic surface wave testing accompanied with our proposed hybrid inverse and poromechanical dispersion model for the assessment and quantitative characterization of permafrost sites. Its applications for early detection and warning systems to monitor infrastructure impacted by permafrost-related geohazards, and to detect the presence of layers vulnerable to permafrost carbon feedback and emission of greenhouse gases into the atmosphere will be the goal of our future studies. Currently, there is no advanced physics-based monitoring system developed for the real-time interpretation of seismic measurements. As such, active and passive seismic measurements can be collected and processed using the proposed hybrid inverse and poromechanical dispersion model for the assessment and quantitative characterization of permafrost sites at various depths in real-time. In the future study, we will focus on the development of an early warning system for the long-term tracking of permafrost conditions. The early warning system can be used to collect seismic measurements and predict the physical and mechanical properties of the foundation permafrost. The system then reports periodic variations in physical (mostly ice content) and mechanical properties of the permafrost being monitored. The same method being applied on different dates (e.g. seasonal basis) can be used to record the change of properties of the permafrost site, and then warn on the degradation of the permafrost exceeding the threshold. The value of the threshold (or critical values) will require more in-depth research to be determined. The early detection and warning systems can be beneficial in monitoring the condition of the foundation permafrost and preventing excessive thawing settlement and significant loss in strength. Similarly, we can detect the presence of peat (based on the physical and mechanical properties) which is vulnerable to permafrost carbon feedback and emission of greenhouse gases into the atmosphere. It's reported that the soils in the permafrost region hold twice as much carbon as the atmosphere does (almost 1,600 billion tonnes) (Schuur et al., 2015). The thawing permafrost can rapidly trigger landslides and erosion. Current climate models assume that permafrost thaws gradually from the surface downwards (Schuur et al., 2015). However, several meters of soil can become destabilized within a few days or weeks instead of a few centimeters of soil thawing each year (Schuur et al., 2015). The missing element of the existing studies and models is that the abrupt permafrost destabilization can occur and contribute to more carbon feedback than the existing models predict as the permafrost degrades.

Reference:

Schuur, E. A., McGuire, A. D., Schädel, C., Grosse, G., Harden, J. W., Hayes, D. J., & Vonk, J. E. (2015). Climate change and the permafrost carbon feedback. Nature, 520(7546), 171-179.

In absence of ground truth for comparison, can you at least quantify the uncertainties of the inverted parameters?

We have selected lower and upper bounds of dispersion spectra to study the uncertainty that propagates through the inversion analysis. The dispersion curve is automatically selected initially based on the highest intensity in the dispersion spectra using MASWave software (Olafsdottir et al., 2018). The uncertainties due to the selection of the dispersion curve from the dispersion spectra have been considered in the revised manuscript. Then a 90% confidence interval, as shown in Figure 2f and 2g, is considered to study the effect of the selection of dispersion curve on the inversion results.

Figure 4a shows the probabilistic distribution of the degree of saturation of unfrozen water with depth in Section 1. Our results show that the active layer has a thickness of about 1.5 m. The predicted permafrost layer (second layer) has a nearly 32% of degree of saturation of unfrozen pore water. Figure 4b shows the degree of saturation of ice with depth. The degree of saturation of ice in the permafrost layer (second layer) ranges from 67% to 79%. Figure 4c illustrates the porosity distribution with depth. The porosity is around 0.60 in the first layer (active layer), from 0.40 to 0.47 in the second layer (permafrost) and from 0.56 to 0.59 in the third layer. Figure 4d and 4e show the predicted mechanical properties of the solid skeletal frame (shear modulus and bulk modulus) in each layer. It was reported by Szymański et al. (2013) that this study site also contains a lot of coarse sandy soils, gravels as well as around 20% silty clay based on the direct sampling methods at the top 15 cm. The predicted shear modulus and bulk modulus for the solid skeletal frame in the permafrost layer (second layer) are about 13 GPa and 12.7 GPa, which are in the range for silty-clayey soils (Vanorio et al. 2003) and are also consistent with the local soil types described by Szymański et al. (2013). The predicted shear modulus and bulk modulus for the solid skeletal frame in the third layer are about 4 GPa and 10 GPa, which are in the range for clayey soils (Vanorio et al. 2003). Figure 4f and 4g show the comparison between the numerical and experimental dispersion relations for R2 and R1 waves, respectively. The numerical predictions show good agreement with the experimental dispersion curves for both R1 and R2 waves. The uncertainty analyses for other Sections are performed in a similar manner.

Reference:

Olafsdottir, E. A., Erlingsson, S., & Bessason, B. (2018). Tool for analysis of multichannel analysis of surface waves (MASW) field data and evaluation of shear wave velocity profiles of soils. Canadian Geotechnical Journal, 55(2), 217-233.

Vanorio, T., Prasad, M., & Nur, A. (2003). Elastic properties of dry clay mineral aggregates, suspensions and sandstones. Geophysical Journal International, 155(1), 319-326.

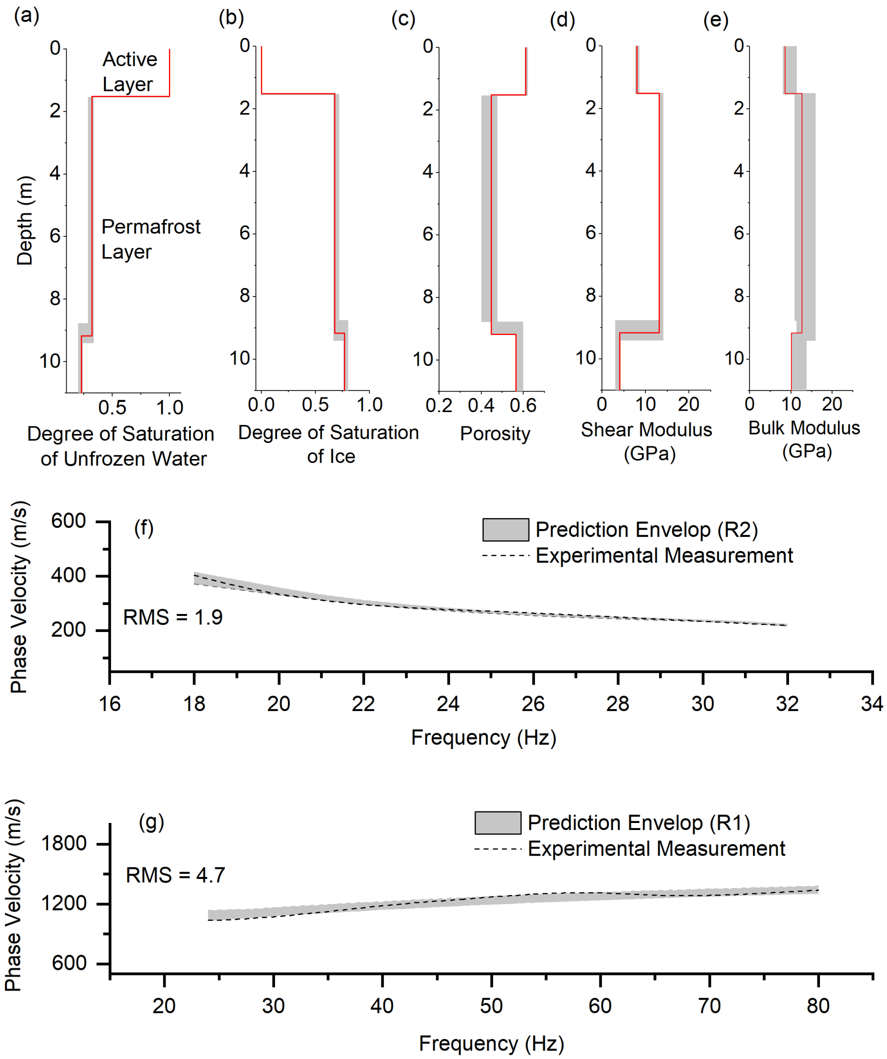

Figure 4: Surface wave inversion results for Section 1: 0m to 120m. **(a)** Degree of saturation of unfrozen water, **(b)** Degree of saturation of ice, **(c)** Porosity distribution, **(d)** Shear modulus of solid skeletal frame, **(e)** Bulk modulus of solid skeletal frame, **(f)** Experimental and numerical dispersion curves for R2 wave, **(g)** Experimental and numerical dispersion curves for R1 wave.

233 " These predictions fit well within the reasonable range of volumetric unfrozen water content for clay or clayey silt". Please provide a reference.

Reference has been provided.

Reference:

Li, Z., Chen, J., & Sugimoto, M. (2020). Pulsed NMR measurements of unfrozen water content in partially frozen soil. Journal of Cold Regions Engineering, 34(3), 04020013.